Available online at www.sciencedirect.com
ScienceDirect
Journal of Molecular Spectroscopy 240 (2006) 26–31
Journal of MOLECULAR SPECTROSCOPY
www.elsevier.com/locate/jms

Laser spectroscopy of the $\tilde{A}^2\Pi$–$\tilde{X}^2\Sigma^+$ 0_0^0 and $\tilde{C}^2\Pi$–$\tilde{A}^2\Pi$ 0_0^0 transitions of SrOD

Shanshan Yu [a], Jin-Guo Wang [a], Phillip M. Sheridan [a], Michael J. Dick [b], Peter F. Bernath [a,b,*]

[a] Department of Chemistry, University of Waterloo, Waterloo, Ont., Canada N2L 3G1
[b] Department of Physics, University of Waterloo, Waterloo, Ont., Canada N2L 3G1

Received 11 July 2006
Available online 12 August 2006

Abstract

High-resolution spectra of SrOD have been recorded using optical-optical double-resonance spectroscopy and laser excitation spectroscopy. SrOD was produced by the reaction of Sr metal vapor and D_2O vapor in a Broida-type oven. The 0_0^0 bands of the $\tilde{A}^2\Pi$–$\tilde{X}^2\Sigma^+$ and $\tilde{C}^2\Pi$–$\tilde{A}^2\Pi$ transitions were observed and rotationally analyzed for the first time. Combined with the previous microwave data from the literature, the present data were fitted using the usual $^2\Sigma^+$ and $^2\Pi$ Hamiltonians, and spectroscopic constants were obtained for the $\tilde{X}^2\Sigma^+$ (000), $\tilde{A}^2\Pi$ (000) and $\tilde{C}^2\Pi$ (000) states of SrOD. An unusually small OH bond length was obtained for the $\tilde{C}^2\Pi$ state, perhaps indicating that the $\tilde{C}^2\Pi$ state of SrOH has a floppy potential similar to the ground state of MgOH.

Keywords: Optical-optical double-resonance; Alkaline-earth monohydroxides

1. Introduction

The spectroscopy of the alkaline earth monohydroxides has been an active topic of discussion in many papers. Their extensive experimental and computational studies have been reviewed by Bernath [1,2] and Ellis [3]. For the SrOH/SrOD free radical, high-resolution studies have been limited to the $\tilde{X}^2\Sigma^+$ ground state and the low-lying $\tilde{A}^2\Pi$ and $\tilde{B}^2\Sigma^+$ excited states. Additional excited states lie high in energy, and as a result high-resolution studies using laser excitation spectroscopy are difficult to perform. We have recently reported on the first high-resolution study of the $\tilde{C}^2\Pi$–$\tilde{A}^2\Pi$ 0_0^0 transition of SrOH using optical-optical double-resonance (OODR) spectroscopy [4]. In the current work we present the first high-resolution study of the $\tilde{C}^2\Pi$–$\tilde{A}^2\Pi$ 0_0^0 transition of SrOD using OODR spectroscopy, as well as the first high-resolution study of the $\tilde{A}^2\Pi$–$\tilde{X}^2\Sigma^+$ 0_0^0 transition of SrOD using laser excitation spectroscopy.

The spectrum of SrOH was first described by Herschel in 1823 [5] who observed band systems centered at 660 and 610 nm. These bands were also observed by Barrow and Caldin [6], but were not identified as arising from SrOH until 1955 when James and Sugden [7] recognized the similarity between the alkaline-earth monohydroxide bands and the alkaline-earth halide bands. No rotational analysis of these bands was reported until 1983 when Nakagawa et al. [8] examined the 0_0^0, 1_1^1 and 2_1^1 bands of the $\tilde{B}^2\Sigma^+$–$\tilde{X}^2\Sigma^+$ transition for both SrOH and SrOD. Later, Brazier and Bernath [9] rotationally analyzed the 0_0^0 band of the $\tilde{A}^2\Pi$–$\tilde{X}^2\Sigma^+$ transition of SrOH using a combination of laser-induced fluorescence and Fourier transform spectroscopy. Additional investigations of vibrationally excited bands of the $\tilde{A}^2\Pi$–$\tilde{X}^2\Sigma^+$ and $\tilde{B}^2\Sigma^+$–$\tilde{X}^2\Sigma^+$ transitions of SrOH were carried out by Presunka and Coxon [10–12] using high-resolution laser excitation spectroscopy. Also Zhao et al. [16] used supersonic jet-cooled molecular beam methods to observe the $\tilde{B}^2\Sigma^+$–$\tilde{X}^2\Sigma^+$ transition of SrOD.

* Corresponding author. Fax: +1 519 746 0435.
E-mail address: bernath@uwaterloo.ca (P.F. Bernath).

0022-2852/$ - see front matter © 2006 Elsevier Inc. All rights reserved.
doi:10.1016/j.jms.2006.08.004

The pure rotational spectra of the ground state of SrOH and SrOD have been examined by Anderson et al. [13] and Fletcher et al. [14,15].

Recently, using low-resolution laser excitation and dispersed fluorescence spectroscopy, Beardah and Ellis [17,18] have located the following five higher energy electronic states for SrOH: $\tilde{B}'^2\Sigma^+$ (25 997 cm^{-1}), $\tilde{C}^2\Pi$ (27 303 cm^{-1}), $\tilde{D}^2\Sigma^+$ (27 698 cm^{-1}), $\tilde{E}^2\Sigma^+$ (29 990 cm^{-1}), and $\tilde{F}^2\Pi$ (32 985 cm^{-1}). Our subsequent OODR study of the $\tilde{C}^2\Pi$–$\tilde{A}^2\Pi$ 0_0^0 transition of SrOH [4] has been the only available high-resolution spectroscopic study on these states.

In the present paper, the 0_0^0 bands of the $\tilde{A}^2\Pi$–$\tilde{X}^2\Sigma^+$ and $\tilde{C}^2\Pi$–$\tilde{A}^2\Pi$ transitions of SrOD have been observed and rotationally analyzed. A total of 364 lines have been measured and assigned for the $\tilde{A}^2\Pi$–$\tilde{X}^2\Sigma^+$ 0_0^0 transition, and 288 lines for the $\tilde{C}^2\Pi$–$\tilde{A}^2\Pi$ 0_0^0 transition. The present data set was combined with the available ground state data from previous work, and a weighted least-squares fit was performed. A complete set of molecular spectroscopic constants has been obtained for the $\tilde{X}^2\Sigma^+$ (000), $\tilde{A}^2\Pi$ (000) and $\tilde{C}^2\Pi$ (000) states of SrOD.

2. Experimental

The SrOD molecules were generated by the reaction of Sr metal vapor and D_2O vapor in a Broida-type oven. Sr metal was resistively heated in a carbon crucible to produce the metal vapor, which was entrained in a flow of ~6 Torr of argon carrier gas. The oxidant gas, D_2O vapor, was admitted to the argon metal-vapor mixture through a ring located above the oven, which was connected to a glass tube containing liquid D_2O at room temperature.

The $\tilde{A}^2\Pi$–$\tilde{X}^2\Sigma^+$ transition was recorded by laser excitation spectroscopy. The output of a cw single-mode ring DCM dye laser (Coherent 699-29) was focused vertically into the reaction chamber of the Broida-type oven. The typical laser power was 400–600 mW in the range of 14 500–14 850 cm^{-1}. As the ring dye laser was scanned, the excitation fluorescence from the $\tilde{A}^2\Pi$ state was collected using a photomultiplier tube (PMT) with a 725 nm red pass filter. Most branches obtained by this way were clear and easily assigned, except for the R_{2ff}, Q_{21fe} and R_{21ee} branches (Fig. 1). These three branches are on the high wavenumber side of the band origin and are probably overlapped with branches from hot bands (e.g., 2_1^1). To simplify the appearance of the spectra, these three branches were also recorded using selective fluorescence detection [8,19]. By scanning the laser through these three branches and monitoring the fluorescence from the connecting P_{21ee}, Q_{2ef} and P_{2ff} branches through a monochromator, the complexity and congestion of the spectrum were much reduced (Fig. 1).

The $\tilde{C}^2\Pi$–$\tilde{A}^2\Pi$ transition was recorded by OODR spectroscopy. The pump laser was a linear cavity dye laser (DCM) with a bandwidth of about 1 cm^{-1}. This laser was used to excite the $\tilde{A}^2\Pi_{\frac{1}{2}}$–$\tilde{X}^2\Sigma^+$ 0_0^0 transition at

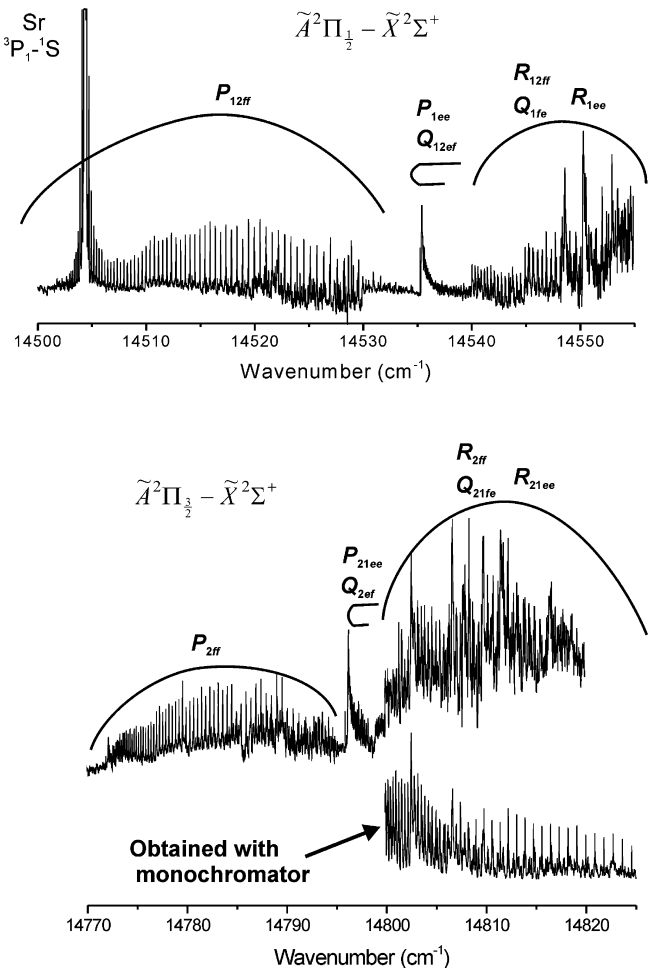

Fig. 1. An overview of the 0_0^0 band of the $\tilde{A}^2\Pi$–$\tilde{X}^2\Sigma^+$ transition of SrOD. The spectra were recorded by scanning the single-mode ring dye laser and monitoring the fluorescence with a 725 nm red pass filter or through a monochromator. All 12 branches for this transition were observed.

14 535 cm^{-1} (the P_{1ee} and Q_{12ef} bandheads) and the $\tilde{A}^2\Pi_{\frac{3}{2}}$–$\tilde{X}^2\Sigma^+0_0^0$ transition at 14 795 cm^{-1} (the P_{21ee} and Q_{2ef} bandheads). The probe laser was a single-mode titanium–sapphire ring laser (Coherent 899-29), which was used to promote the SrOD molecules from the $\tilde{A}^2\Pi$ state to the $\tilde{C}^2\Pi$ state. Because there was no low-resolution work on the high-lying states of SrOD, the probe laser wavenumbers for each spin-orbit component of the $\tilde{C}^2\Pi$–$\tilde{A}^2\Pi$ transition were chosen based on the corresponding transition of SrOH in our previous work [4]. The output of the pump and probe lasers were directed collinearly and focused into the reaction chamber of the Broida-type oven. The signal was optimized by maximizing the overlap of the pump and probe lasers in the reaction zone. As the probe laser was scanned, the excitation fluorescence from the $\tilde{C}^2\Pi$ state was collected using a PMT with a 500 nm blue pass filter. The probe laser scanned the 12 690–12 805 cm^{-1} region for the $\tilde{C}^2\Pi_{\frac{1}{2}}$–$\tilde{A}^2\Pi_{\frac{1}{2}}$ transition and the 12 450–12 600 cm^{-1} region for the $\tilde{C}^2\Pi_{\frac{3}{2}}$–$\tilde{A}^2\Pi_{\frac{3}{2}}$ transition.

In both experiments, a small fraction of the single-mode laser beam was directed into an I_2 cell. The laser excitation

spectra of I_2 [20] were recorded simultaneously to calibrate the line positions of the $\tilde{A}^2\Pi$–$\tilde{X}^2\Sigma^+$ transition and the absorption spectra of I_2 [21] were recorded simultaneously to calibrate the line positions of the $\tilde{C}^2\Pi$–$\tilde{A}^2\Pi$ transition. The accuracy of our SrOD line positions is approximately 0.005 cm^{-1}.

3. Results and discussion

Fig. 1 shows an overview spectrum of the $\tilde{A}^2\Pi$–$\tilde{X}^2\Sigma^+$ 0_0^0 transition obtained by laser excitation spectroscopy. The spin-orbit splitting of the $\tilde{A}^2\Pi$ (000) state in SrOD is found to be very close to that in SrOH (260 cm^{-1}), therefore the two subbands of the $\tilde{A}^2\Pi$–$\tilde{X}^2\Sigma^+$ 0_0^0 transition are well separated. The program Wavereader, written by Wu et al. (East China Normal University), was used to determine the line positions, and a color Loomis–Wood program was used to pick out the branches. Each of the subbands consists of six branches, P_{ff}, P_{ee}, Q_{ef}, R_{ff}, Q_{fe}, and R_{ee}, which are spaced approximately by $-3B$, $-B$, $-B$, $+B$, $+B$ and $+3B$, respectively. Transitions in all 12 branches were observed and rotationally assigned. The $-B$ branches give rise to strong bandheads at J of around 30 and the $-3B$ branches give rise to weak bandheads at J of around 80. The two $-B$ branches (P_{ee} and Q_{ef}) and the two $+B$ branches (R_{ff} and Q_{fe}) are separated by the ground state spin-rotation interaction, respectively. The spin-rotation splitting in the ground state is resolved starting at $J'' = 15.5$. Fig. 2 shows an expanded view of the R_{2ff}, Q_{21fe} and R_{21ee} branches. Rotational assignments were made using lower state combination differences [13].

The rotational transitions observed for the $\tilde{A}^2\Pi$–$\tilde{X}^2\Sigma^+$ 0_0^0 transition of SrOD were fitted together using a weighted nonlinear least-squares procedure. The energy levels of the $\tilde{X}^2\Sigma^+$ (000) and $\tilde{A}^2\Pi$ (000) states of SrOD were calculated using the usual $\hat{N}^2$ Hamiltonian of Brown et al. [22] with matrix elements derived using Hund's case (a) basis functions. An explicit listing of these matrix elements is provided by Douay et al. [23] (for $^2\Sigma^+$ states) and Amiot et al. (for $^2\Pi$ states) [24]. The results of this fit provided combination differences for the $\tilde{A}^2\Pi$ (000) state of SrOD, which were used for the rotational assignments in the 0_0^0 band of the $\tilde{C}^2\Pi$–$\tilde{A}^2\Pi$ transition.

Fig. 3 shows an overview of the 0_0^0 band of the $\tilde{C}^2\Pi$–$\tilde{A}^2\Pi$ transition in SrOD recorded by OODR spectroscopy. Each spectrum exhibits a clear P, Q, and R structure. Because $\Delta\Lambda = 0$ for the $\tilde{C}^2\Pi$–$\tilde{A}^2\Pi$ transition, the Q branch lines are weak [25]. Fig. 4 shows an expanded view of the $\tilde{C}^2\Pi_{\frac{1}{2}}$–$\tilde{A}^2\Pi_{\frac{1}{2}}$ 0_0^0 transition. Because the pump laser was set to excite the P_{1ee}, Q_{12ef} (at 14 535 cm^{-1}) and P_{21ee}, Q_{2ef} (at 14 795 cm^{-1}) bandheads of the $\tilde{A}^2\Pi$–$\tilde{X}^2\Sigma^+$ 0_0^0 transition, e parity levels were predominately populated in the $\tilde{A}^2\Pi$ (000) state. As a result, the P_{ee} and R_{ee} branches of the $\tilde{C}^2\Pi$–$\tilde{A}^2\Pi$ 0_0^0 transition are more intense than the P_{ff} and R_{ff} branches, and the Q_{ef} branches for both spin components were not observed in our experiment. The rotational assignments of the P_{ee}, R_{ee}, P_{ff} and R_{ff} branches were made

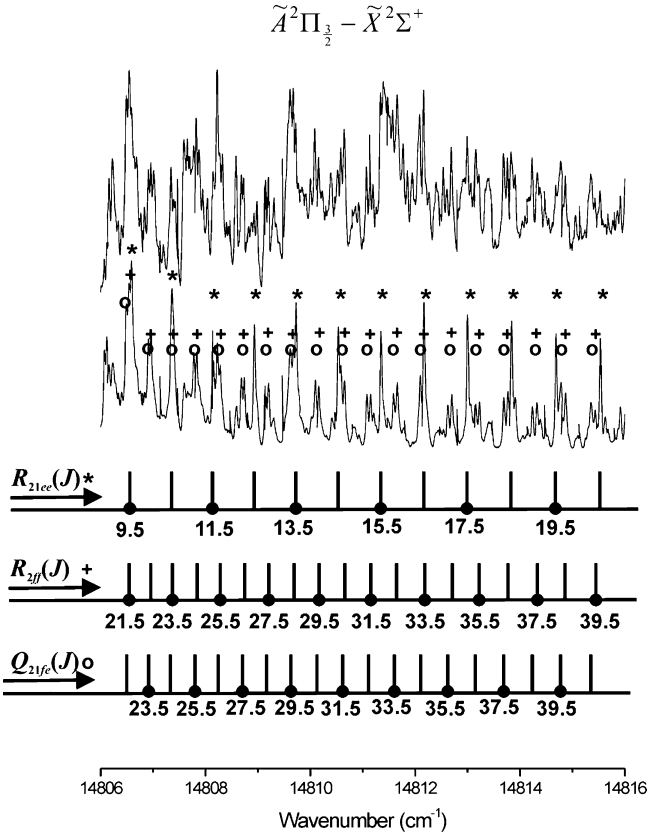

Fig. 2. An expanded view of the R_{21ee}, R_{2ff} and Q_{21fe} branches of the 0_0^0 band of the $\tilde{A}^2\Pi$–$\tilde{X}^2\Sigma^+$ transition of SrOD. The top spectrum was obtained by scanning the single-mode ring dye laser and monitoring the fluorescence with a 725 nm red pass filter, and the bottom spectrum was obtained by scanning the single-mode ring dye laser and monitoring the fluorescence through a monochromator. The R_{2ff} and Q_{21fe} branches are split by the spin-rotation interaction in the ground state, which is resolved starting at $J = 15.5$.

using lower state combination differences in the $\tilde{A}^2\Pi$ (000) state. Assignments in the weak Q_{fe} branches were made by predictions using the R_{ff} lines and the energy differences between the e and f levels in the $\tilde{A}^2\Pi$ (000) state.

Additional weak bands were also observed in our OODR experiments, one of which was observed with a band origin of around 12 713 cm^{-1} and the lower state was confirmed to be the $\tilde{A}^2\Pi_{\frac{1}{2}}$ (000) state by lower state combination differences. Only the R_{ee} and P_{ee} branches (J'' from 5.5 to 36.5) were rotationally assigned for this band. Another band was observed with a band origin of around 12 586 cm^{-1} and the lower state was confirmed to be the $\tilde{A}^2\Pi_{\frac{3}{2}}$ (000) state. Only the R_{ee} and P_{ee} branches (J'' from 5.5 to 36.5) were rotationally assigned for this band. Because only two branches were assigned for these two bands, we do not have enough information to determine their upper states. Beardah and Ellis [18] observed the $\tilde{B}'^2\Sigma^+$ state of SrOH with an energy of 25 997 cm^{-1}. The $\tilde{A}^2\Pi_{\frac{1}{2}}$ (000) and $\tilde{A}^2\Pi_{\frac{3}{2}}$ (000) states of SrOD have an energy of 14 537 and 14 799 cm^{-1}, respectively. The 0_0^0 bands of the $\tilde{B}'^2\Sigma^+$–$\tilde{A}^2\Pi_{\frac{1}{2}}$ and $\tilde{B}'^2\Sigma^+$–$\tilde{A}^2\Pi_{\frac{3}{2}}$ transitions would be located at 11 460 and 11 198 cm^{-1}, respectively.

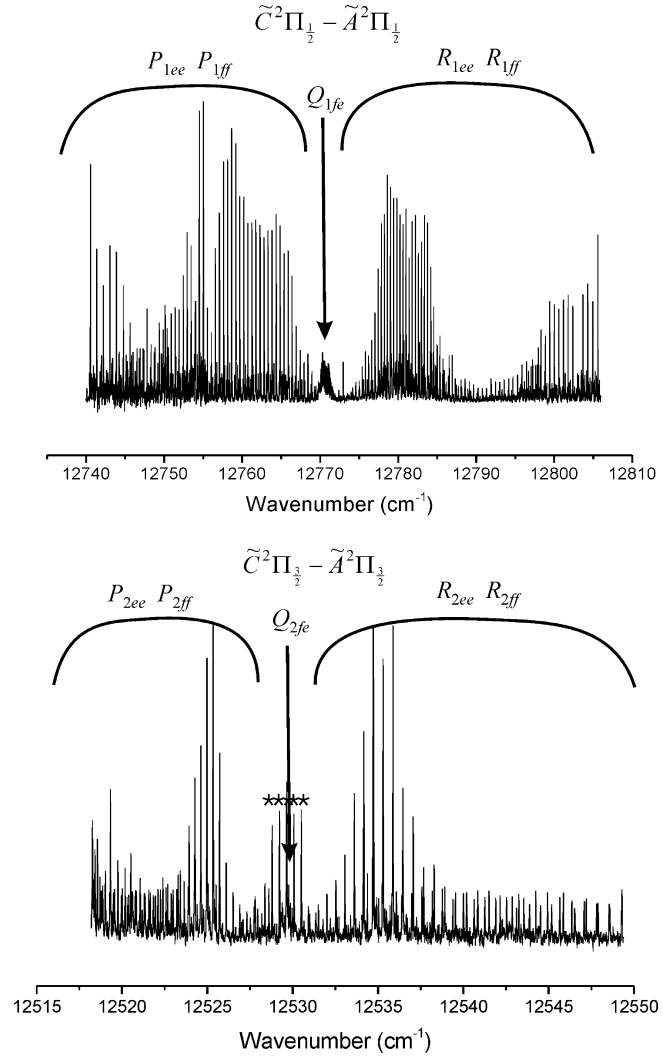

Fig. 3. An overview of the 0_0^0 band of the $\tilde{C}^2\Pi$–$\tilde{A}^2\Pi$ transition of SrOD recorded by OODR spectroscopy. Both spectra exhibit a double P and double R structure and the intensity pattern in the P and R branches results from the various J levels populated in the $\tilde{A}^2\Pi$ state by the pump laser. The Q branches for the both spin components are weak. Strong lines located near the Q_{2fe} branch, indicated by asterisks, are probably due to an excited vibrational band.

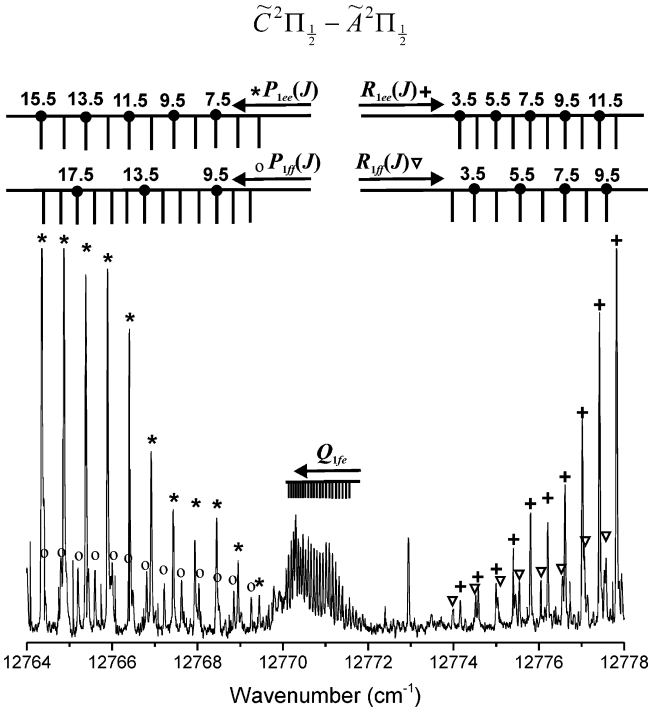

Fig. 4. An expanded view of the 0_0^0 band of the $\tilde{C}^2\Pi_{\frac{1}{2}}$–$\tilde{A}^2\Pi_{\frac{1}{2}}$ transition of SrOD recorded by OODR spectroscopy. The pump laser was fixed to excite the heads of the P_{1ee} and Q_{12ef} branches of the $\tilde{A}^2\Pi - \tilde{X}^2\Sigma^+ 0_0^0$ transition, therefore e parity levels were predominately populated in the $\tilde{A}^2\Pi$ state. As a result, the P_{1ee} and R_{1ee} branches are more intense than the P_{1ff} and R_{1ff} branches, and the Q_{1ef} branch was not observed in our experiments. The Λ-doubling splitting is resolved at very low J values.

The Sr–O stretching mode (ν_3) and the Sr–O–D bending mode (ν_2) in the ground state of SrOD were determined to be 517 and 282 cm^{-1}, respectively [2,8,16]. The combination bands $2_0^3 3_0^1$ and $2_0^1 3_0^2$ of the $\tilde{B}'^2\Sigma^+$–$\tilde{A}^2\Pi_{\frac{1}{2}}$ and $\tilde{B}'^2\Sigma^+$–$\tilde{A}^2\Pi_{\frac{3}{2}}$ transitions are expected to be at around 12800 and 12500 cm^{-1}. We therefore tentatively assign the two unknown upper states as the (012) and (031) levels of the $\tilde{B}'^2\Sigma^+$ state.

Finally, a simultaneous least-squares fit was performed, which included the present $\tilde{A}^2\Pi$–$\tilde{X}^2\Sigma^+ 0_0^0$ and $\tilde{C}^2\Pi$–$\tilde{A}^2\Pi$ 0_0^0 data, as well as the pure rotational transitions measured in the microwave study of the $\tilde{X}^2\Sigma^+$ (000) state [13]. The output file of this fit is provided in the Supplementary Table S1. An estimated uncertainty of 0.005 cm^{-1} was used for most lines obtained in this work and an uncertainty of 10^{-6} cm^{-1} for the millimeter-wave transitions. Local perturbations were observed at $J = 30.5$ for both e and f levels of the $\tilde{C}^2\Pi_{\frac{1}{2}}$ (000) state and at $J = 23.5$ for both e and f levels of the $\tilde{C}^2\Pi_{\frac{3}{2}}$ (000) state, and the perturbed lines were simply deweighted in our fit.

The spectroscopic constants obtained for SrOD are provided in Table 1. In our fit, the absolute energy of the 000 level of the $\tilde{X}^2\Sigma^+$ ground state was fixed at zero. The obtained origins for the $\tilde{A}^2\Pi$ (000) and $\tilde{C}^2\Pi$ (000) states are 14668.07360 (40) cm^{-1} and 27318.88299 (62) cm^{-1} relative to this level, respectively. From our previous paper on SrOH [4], the origins for the $\tilde{A}^2\Pi$ (000) and $\tilde{C}^2\Pi$ (000)

Table 1
Hund's case (a) constants (in cm^{-1}) for the $\tilde{X}^2\Sigma^+$, $\tilde{A}^2\Pi$ and $\tilde{C}^2\Pi$ states of SrOD[a]

Constant	$\tilde{X}^2\Sigma^+$ (000)	$\tilde{A}^2\Pi$ (000)	$\tilde{C}^2\Pi$ (000)
T	0.0	14668.07360 (40)	27318.88299 (62)
B	0.225316156 (14)	0.22932627 (53)	0.2316110 (15)
$D/10^{-7}$	1.66514 (14)	1.6579 (12)	2.3965 (64)
$\gamma/10^{-3}$	2.20143 (32)	—	—
A	—	262.52710 (51)	19.5525 (11)
$A_D/10^{-4}$	—	—	−3.087 (22)
p	—	−0.130107 (28)	−0.032380 (51)
$q/10^{-4}$	—	−1.361 (40)	−8.923 (16)

[a] All uncertainties are 1σ.

states are 14674.04171 (39) cm^{-1} and 27307.24754 (66) cm^{-1} relative to the 000 level of the $\tilde{X}^2\Sigma^+$ ground state of SrOH, respectively. The differences between the origins are approximately 10 cm^{-1}. An A_D term was required for the $\tilde{C}^2\Pi$ (000) state to successfully model the data, which is probably due to the local perturbations observed in different e and f levels in the $\tilde{C}^2\Pi$ (000) state. All the other constants are comparable to those for SrOH except for the $\tilde{C}^2\Pi$ (000) state spin-orbit constant. For the $\tilde{A}^2\Pi$ (000) state, A value of 262.52710 (51) cm^{-1} was obtained for SrOD and 263.58782 (61) cm^{-1} for SrOH. However, for the $\tilde{C}^2\Pi$ (000) state, a value of 19.5525 (11) cm^{-1} was obtained for SrOD and 24.6607 (11) cm^{-1} for SrOH. At this moment, we do not have enough information to explain the discrepancy in the $\tilde{C}^2\Pi$ state spin-orbit constants of SrOH and SrOD. Evidently there are local and global perturbations in the $\tilde{C}^2\Pi$ state that are different for SrOH and SrOD.

As noted in our previous work [4], there is a remarkable difference in the value of the spin-orbit constant between the $\tilde{A}^2\Pi$ (000) and $\tilde{C}^2\Pi$ (000) states, which can be attributed to the molecular orbital character of the unpaired electron [4]. The molecular spin-orbit constant A can be represented by a linear combination of the atomic spin-orbit coupling constants, whose coefficients are the orbital mixing percentages. The Sr atomic spin-orbit coupling constants are 534 cm^{-1} for $5p\pi$ orbital, 112 cm^{-1} for the $4d\pi$ orbital, 192 cm^{-1} for the $6p\pi$ orbital and 30 cm^{-1} for the $5d\pi$ orbital [26]. The molecular orbital of the unpaired electron in the $\tilde{A}^2\Pi$ state has large mixing percentages of the $5p\pi$ and $4d\pi$ atomic orbitals while the molecular orbital in the $\tilde{C}^2\Pi$ state has small mixing percentages of the $5p\pi$ and $4d\pi$ orbitals and large mixing percentages of higher energy orbitals, which results in a much smaller spin-orbit constant in the $\tilde{C}^2\Pi$ state.

The obtained B_0 constants allowed us to calculate the r_0 bond lengths for the $\tilde{A}^2\Pi$ and $\tilde{C}^2\Pi$ states. Table 2 lists the r_0 bond lengths for the $\tilde{X}^2\Sigma^+$, $\tilde{A}^2\Pi$, $\tilde{B}^2\Sigma^+$ and $\tilde{C}^2\Pi$ states of SrOH. A value of 0.822 Å was determined for the OH bond length in the $\tilde{C}^2\Pi$ state, which appears unusually small for a rigidly linear molecule. A $^2\Pi$ Hamiltonian successfully fits the experimental data, suggesting that SrOH is linear or very nearly linear in its $\tilde{C}^2\Pi$ state. The unusually small OH bond length perhaps indicates that the $\tilde{C}^2\Pi$ state of SrOH has a floppy bending potential similar to the ground state of MgOH [27]. The ground state of MgOH has an OH r_0 bond length of 0.871 Å [27]. Alternately, the global perturbations of the $\tilde{C}^2\Pi$ state that have resulted in different A values for SrOH and SrOD may also have given different non-mechanical contributions to the B values. These perturbed B values would then result in anomalous bond lengths.

Table 2
Bond lengths (Å) for SrOH

	$\tilde{X}^2\Sigma^+$[a]	$\tilde{A}^2\Pi$[b]	$\tilde{B}^2\Sigma^+$[c]	$\tilde{C}^2\Pi$[b]
r_0 (SrO)	2.111	2.091	2.098	2.096
r_0 (OH)	0.922	0.922	0.921	0.822

[a] Determined from millimeter-wave data of SrOH, SrOD and ^{86}SrOH [13].
[b] Determined from optical data of SrOH [4] and SrOD (this work).
[c] Determined from optical data of SrOH and SrOD [8].

In conclusion, the $\tilde{A}^2\Pi$–$\tilde{X}^2\Sigma^+$ and $\tilde{C}^2\Pi$–$\tilde{A}^2\Pi$ transitions of SrOD have been recorded using laser excitation and optical-optical double-resonance spectroscopy. The 0_0^0 bands of the two transitions were observed and rotationally analyzed for the first time. The present data were fitted together with the previous microwave data from the literature, and spectroscopic constants were obtained for the $\tilde{X}^2\Sigma^+$ (000), $\tilde{A}^2\Pi$ (000) and $\tilde{C}^2\Pi$ (000) states of SrOD. An unusually small OH bond length was obtained for the $\tilde{C}^2\Pi$ state, perhaps indicating that the $\tilde{C}^2\Pi$ state of SrOH has a floppy bending potential similar to the ground state of MgOH.

Acknowledgment

Funding for this work was provided by the Natural Sciences and Engineering Research Council (NSERC) of Canada.

Appendix A. Supplementary data

Supplementary data for this article are available on ScienceDirect (www.sciencedirect.com) and as part of the Ohio State University Molecular Spectroscopy Archives (http://msa.lib.ohio-state.edu/jmsa_hp.htm).

References

[1] P.F. Bernath, Science 254 (1991) 665–670.
[2] P.F. Bernath, Adv. Photochem. 23 (1997) 1–62.
[3] A.M. Ellis, Int. Rev. Phys. Chem. 20 (2001) 551–590.
[4] J.-G. Wang, P.M. Sheridan, M.J. Dick, P.F. Bernath, J. Mol. Spectrosc. 236 (2006) 21–28.
[5] J.F.W. Herschel, Trans. Roy. Soc. Edinburg 9 (1823) 445–460.
[6] R.F. Barrow, E.F. Caldin, Proc. Phys. Soc. B 62 (1948) 32–39.
[7] C.G. James, T.M. Sugden, Nature (London) 175 (1955) 333–334.
[8] J. Nakagawa, R.F. Wormsbecher, D.O. Harris, J. Mol. Spectrosc. 97 (1983) 37–64.
[9] C.R. Brazier, P.F. Bernath, J. Mol. Spectrosc. 114 (1985) 163–173.
[10] P.I. Presunka, J.A. Coxon, Can. J. Chem. 71 (1993) 1689–1705.
[11] P.I. Presunka, J.A. Coxon, J. Chem. Phys. 101 (1994) 201–222.
[12] P.I. Presunka, J.A. Coxon, Chem. Phys. 190 (1995) 97–111.
[13] M.A. Anderson, W.L. Barclay Jr., L.M. Ziurys, Chem. Phys. Lett. 196 (1992) 166–172.
[14] D.A. Fletcher, K.Y. Jung, C.T. Scurlock, T.C. Steimle, J. Chem. Phys. 98 (1993) 1837–1842.
[15] D.A. Fletcher, M.A. Anderson, W.L. Barclay Jr., L.M. Ziurys, J. Chem. Phys. 102 (1995) 4334–4339.
[16] C. Zhao, P.G. Hajigeorgiou, P.F. Bernath, J.W. Hepburn, J. Mol. Spectrosc. 176 (1996) 268–273.
[17] M.S. Beardah, A.M. Ellis, J. Chem. Phys. 110 (1999) 11244–11254.
[18] M.S. Beardah, A.M. Ellis, J. Mol. Spectrosc. 218 (2003) 80–84.
[19] C. Linton, J. Mol. Spectrosc. 69 (1978) 351–364.
[20] S. Gerstenkorn, P. Luc, Atlas du spectre d'Absorption de la Molécule d'Iode (Laboratorie Aimé-Cotton, CNRS 91405, Orsay, France, 1978).
[21] S. Gerstenkorn, J. Verges, J. Chevillard, Atlas du spectre d'Absorption de la Molécule d'Iode (Laboratorie Aimé-Cotton, CNRS 91405, Orsay, France, 1982).

[22] J.M. Brown, E.A. Colbourn, J.K.G. Watson, F.D. Wayne, J. Mol. Spectrosc. 74 (1979) 294–318.
[23] M. Douay, S.A. Rogers, P.F. Bernath, Mol. Phys. 64 (1988) 425–436.
[24] C. Amiot, J.-P. Maillard, J. Chauville, J. Mol. Spectrosc. 87 (1981) 196–218.
[25] G. Herzberg, Molecular Spectra and Molecular Structure, vol. 1, Krieger, Malabar, Florida, 1989.
[26] C.E. Moore, Atomic Energy Levels, NSRDS Natl. Bur. Stand. No. 35, U.S. GPO, Washington, DC, 1971, p. 192.
[27] A.J. Apponi, M.A. Anderson, L.M. Ziurys, J. Chem. Phys. 111 (1999) 10919–10925.